

# Improved Performance of CEA Microbial Fuel Cells with Increased Reactor Size

Yanzhen Fan<sup>a</sup>, Sun-Kee Han<sup>a,b</sup>, Hong Liu<sup>\*a</sup>*Received (in XXX, XXX) Xth XXXXXXXXX 200X, Accepted Xth XXXXXXXXX 200X*

DOI: 10.1039/b000000x

The performance of an over 10 times larger microbial fuel cell (MFC) with double cloth electrode assembly (CEA) during 63 days of continuous operation demonstrates that the excellent performance of CEA-MFC can be further improved during scale-up. With a new separator material and U-shaped current collectors, the larger MFC produced a maximum power density of  $4.30 \text{ W m}^{-2}$  at a current density of  $16.4 \text{ A m}^{-2}$ , corresponding to a volumetric power density of  $2.87 \text{ kW m}^{-3}$  at  $10.9 \text{ kA m}^{-3}$  for a double CEA-MFC. The high current density led to a high average coulombic efficiency (CE) of 83.5% as well as a high potential COD removal rate of  $93.5 \text{ kg m}^{-3} \text{ d}^{-1}$ . Energy efficiency is estimated in the range of 21–35%, depending on the operating voltage. The low-cost non-woven cloth separator further reduced the anode-cathode spacing and internal resistance, greatly enhancing the power generation. The enhanced self-production of bicarbonate buffer, which can be manipulated by adjusting hydraulic retention time and substrate concentration, also contributed to the improved performance. The results demonstrate the great potential of MFC technology in competing with methanogenic anaerobic digestion for waste-to-electricity and wastewater treatment.

## Introduction

The finite reserves of fossil fuels and ever-increasing pressure on reducing greenhouse gas emission have generated an urgent need for alternative sources of energy. Wastewater treatment accounts for about 3% of electrical energy consumed in U.S and other developed countries.<sup>1</sup> It is estimated that wastewater contains as much as 9.3 times the amount of energy currently consumed to treat the water in a modern wastewater treatment plant.<sup>2</sup> Microbial fuel cell (MFC) technology, which uses microorganisms to catalyze the direct generation of electricity from biodegradable organic matter, provides a completely new approach for energy generation from wastewater while accomplishing wastewater treatment simultaneously.<sup>3</sup> MFC technology holds great promise in converting wastewater treatment from an energy consumer to a net energy producer, thus drastically enhancing energy sustainability for wastewater treatment and reuse.

MFCs have drawn much research attention in the last decade, especially after the demonstration of direct harvesting of electricity from wastewater.<sup>4</sup> Relatively low power density is the greatest challenge for practical application of MFC technology for wastewater treatment. Extensive studies have led to an increase in power density by several orders of magnitude in less than 10 years. Maximum power densities of air cathode MFCs have reached  $1.55 \text{ kW m}^{-3}$ .<sup>5</sup> However, great challenges in further increasing power density have had a plateauing effect on attainable power outputs of MFCs.

Scale-up is an important issue for practical application of MFCs, especially in the field of wastewater treatment. Maintaining performance during scale-up has proven to be challenging.<sup>6</sup> Air-cathode MFCs hold a greater promise for practical applications due to the fact that oxygen is the only ubiquitous and virtually free electron acceptor. However, the volumes of most air-cathode MFCs studied have been relatively small. MFCs with cloth electrode assemblies (CEAs) produced a

## Broader context

Maintaining performance during scale-up of MFCs is an important but challenging issue. A major reason for decreased performance during scale-up is the enlarged anode-cathode spacing. This study demonstrates the inherent advantage of CEA structure in maintaining performance during scale-up. The oxygen tolerant anodic microbial community, enabled faster reactor start-up and allowed for the use of thinner separator material. The thinner, durable low-cost separator halved the anode-cathode spacing and led to more than doubled power density. Compared with anaerobic digestion for wastewater treatment, MFCs could have a similar energy efficiency, higher COD loading rate and electricity generation rate, and better effluent quality at an affordable capital cost. The results demonstrate the great potential of MFC technology in self-sufficient wastewater treatment and renewable electricity generation.

high power density of  $1.55 \text{ kW m}^{-3}$ , but the liquid volume was only 2.5 ml.<sup>5</sup> Several liter-scale air cathode MFCs have been developed with liquid volume in the range of 1 to 20 L, or 2-4 orders of magnitude larger than the ml-scale MFC.<sup>7, 8, 9, 10, 11</sup> The maximum power densities of these liter-scale MFCs, however, are in the range of  $0.17$  to  $11 \text{ W m}^{-3}$ , which were 2-4 orders of magnitude lower than the ml-scale MFCs with power densities over  $1 \text{ kW m}^{-3}$ .<sup>5,12</sup> Therefore, increasing reactor size from ml-scale to liter-scale doesn't necessarily lead to a significant increase in total power output. The primary aim of MFC scale-up is not just to increase reactor size but to increase total power and current output. Determining if the excellent performance of CEA-MFC can be maintained or even enhanced during scale-up is of great interest.

A CEA-MFC, over 10 times larger than those previously reported<sup>12</sup>, was constructed and continuously operated for 63 days. The use of a new separator material, U-shape Ti current collectors, an oxygen tolerant microbial community, and improved operating conditions resulted in a further improvement in MFC performance. The potential application of MFC technology in competing with methanogenic anaerobic digestion for waste-to-electricity and wastewater treatment is also re-evaluated.

## Experimental

### Design and construction of the large CEA-MFC

A Single chamber air-cathode MFC with a double CEA was constructed based on the smaller MFC previously described.<sup>12</sup> To summarize, a non-woven fabric layer (Armo Style # 6000) was sandwiched between the carbon cloth anode (CCP, fuelcellearth.com) and the carbon cloth/Pt/PTFE cathode (20% of Pt/C catalyst; E-TEK, USA) to form a CEA. U-shape Ti wires were used as the anode and cathode current collectors in both CEAs. The two CEAs were placed in between three identical 0.6 cm thick acrylic frames with 5 cm x 20 cm openings to form a five-layer sandwich structure, with CEA1 at the top and CEA2 at the bottom of the reactor initially. Three 1 cm by 1 cm crosses were cut through the anode and cloth layers of CEA1, evenly distributed along the long axis, to release the possible biogas produced between the anode and cathode. Alternatively, for CEA2, three holes ( $\Phi 0.3 \text{ cm}$ ) were punched through the two layers to allow venting of possible biogas. The reactor has a liquid volume of 30 ml and a total effective surface area of  $200 \text{ cm}^2$ . Figure 1 shows the photo and assembly schematics for the double CEA-MFC.

### CEA-MFC Operation

The MFC was inoculated with a mixed bacterial culture from the anode of an air cathode MFC, which was originally inoculated with domestic wastewater from the Corvallis Wastewater Treatment Plant (Corvallis, OR) and was operated for more than 3 years using acetate. Unless otherwise specified, acetate (100 mM) was used as the substrate. and the medium solution contained the following (per liter):  $\text{NH}_4\text{Cl}$ , 1.5 g;  $\text{KCl}$ , 0.13 g;  $\text{NaH}_2\text{PO}_4 \cdot \text{H}_2\text{O}$ , 5.84 g;  $\text{Na}_2\text{HPO}_4 \cdot 7\text{H}_2\text{O}$ , 15.5 g; and mineral (12.5 ml) and vitamin (12.5 ml) solutions as reported.<sup>13</sup> The MFC experiments were operated at  $32 \pm 1^\circ \text{C}$  in a temperature-controlled chamber.

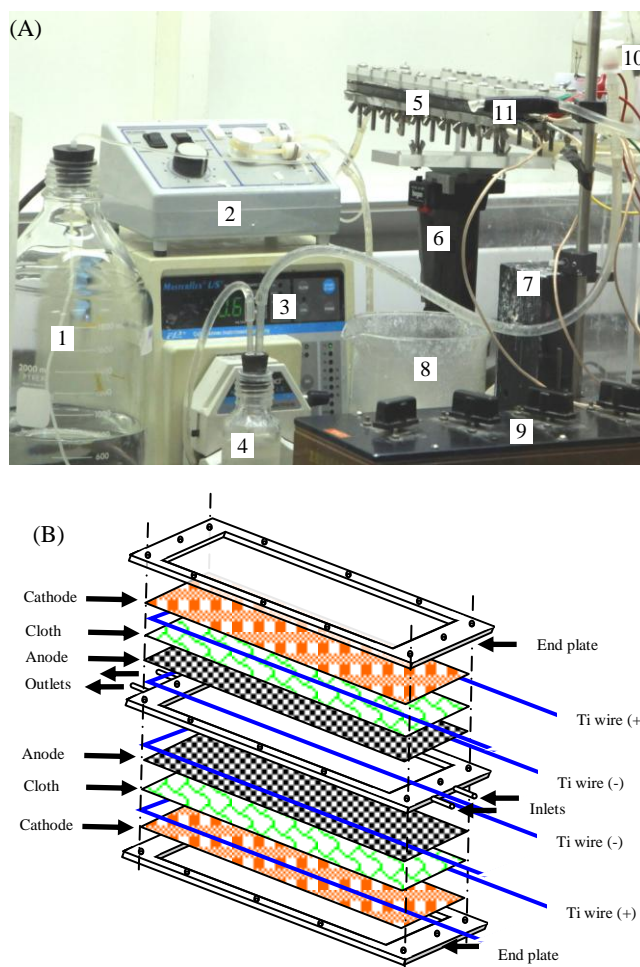


**Fig. 1** (A) A photo of the experimental setup testing the large MFC. 1. Feed bottle, 2. Feed pump, 3. Recirculation pump (optional), 4. Recirculation bottle, 5. Larger reactor, 6. Tilt angle adjusting device for the reactor, 7. Outlets level control device, 8. Effluent reservoir, 9. Precision resistor box, 10. Gas sampling port, 11. Effluent outlet. (B) Schematic of the large reactor with double cloth-electrode-assemblies.

The double CEA-MFC was inclined at an angle of  $5^\circ$  with CEA-1 on the top and CEA-2 at the bottom initially. Batch mode was initially employed and the system was switched to the continuous flow mode after two days as power output started to increase significantly. Then the CEA-MFCs were continuously fed at a flow rate of  $0.4 \text{ ml/min}$  maintained through a peristaltic pump, corresponding to a hydraulic retention time (HRT) of  $1.2 \text{ h}$ . The medium solution in a 2000 ml bottle was autoclaved before being fed to the MFC at the lower end of the reactor. A portion of the effluent was recirculated back to the influent with another peristaltic pump at a flow rate of  $20 \text{ ml/min}$  to achieve more even distribution of the medium solution. A 50 ml bottle was included in the recirculation line to collect the possible gas produced in the MFC.

The MFC was considered to be started-up when the voltage output stabilized within about a week. Once start-up was achieved, the effects of water pressure (from the 2<sup>nd</sup> to the 4<sup>th</sup> week), HRT (from the 5<sup>th</sup> week to the 6<sup>th</sup> week), and recirculation (the 6<sup>th</sup> week) were investigated. Water pressure was controlled by finely adjusting the level of the silicone tube outlet level via a screw drive mechanism. The effluent water level was adjusted

from -4 cm to +4 cm in the following sequence: 0 cm, +1 cm, -1 cm, +2 cm, -4 cm, +4 cm, -2 cm, 0 cm, before the reactor was flipped to study the difference between the top CEA and the bottom CEA. The various HRTs (0.37-3.4 h) were adjusted by varying the flow rate from 0.15 to 1.3 ml/min, with actual flow rate calculated based on daily medium consumption. The effect of recirculation on MFC performance was investigated by adding or removing the 50 ml recirculation bottle.

From the 7<sup>th</sup> week, the effect of phosphate buffer concentration (0.05 M, 0.1 M and 0.2 M) on MFC performance was investigated. The flow rate and acetate concentration were also varied to study the effect of self-produced bicarbonate on MFC performance. The recirculation bottle was removed during this period of research.

## Analyses

Both CEAs of the MFC were separately connected to a precision decade resistance box with a resolution and minimum resistance of 0.1  $\Omega$  (602-N, General Radio). Voltage (V) was recorded, using a multichannel data acquisition system (2700, Keithly, USA), and used to calculate the volumetric power density, based on liquid reactor volume (30 ml), and surface power density, based on projected surface area of the electrode (100 cm<sup>2</sup> for each CEA and 200 cm<sup>2</sup> for the reactor). The contact and wiring resistances (about 0.06  $\Omega$ ) were considered in calculation of current (I) and calculated by measuring both voltages over the resistance box terminals and over the current collector (Ti wire) terminals.

For the preparation of polarization curves, the MFC was first stabilized for about 30 min at 10 k $\Omega$ . The external resistances of both CEAs were then simultaneously reduced with a typical sequence of 100, 50, 20, 10, 5, 3, 2.4, 2, 1.6, 1.4, 1.2, 1.0  $\Omega$  to reduce the voltage to about 0.2 V. At each resistance, MFCs ran for about 20 min to ensure stable power output had been achieved. It took approximately 4 h of operation to finish a polarization curve. The internal resistance of each CEA,  $R_{int}$ , was calculated from the linear parts of the I-V polarization curves. Area specific resistances ( $\Omega$  cm<sup>2</sup>) were also calculated, by multiplying the internal resistance ( $\Omega$ ) by the projected electrode area (cm<sup>2</sup>), for comparison with other studies. More information on preparation of polarization curves and discussion on power overestimation can be found in Supplementary Information.

Acetate concentrations in both influent and effluent were analyzed with an Agilent 1000 series high performance liquid chromatography (Agilent Technologies, Santa Clara, CA) equipped with an RID detector and an Aminex HPX-87H column (Bio-Rad Laboratories, Hercules, CA). A solution of 5 mM per liter H<sub>2</sub>SO<sub>4</sub> was used as the running buffer at a flow rate of 0.6 ml/min. Coulombic efficiency (CE) was calculated based on the ratio of the average current, one-hour before taking acetate samples, and the theoretical current, calculated based on the amount of acetate removed.

When there was noticeable biogas production, indicated by the gas buildup in the recirculation bottle, 100  $\mu$ l of gas was withdrawn, using a syringe, from the gas sampling port located at the outlet of the reactor. The gas sample was immediately injected into a gas chromatograph (Agilent 6890; J&W Scientific, USA) for the analysis of gas composition. The GC was equipped with a thermal conductivity detector and a column (113-3133

CARBONPLT, 30m  $\times$  0.32 mm  $\times$  3  $\mu$ m, J&W Scientific, USA) with argon as the carrier gas.

## Results

### Start-up of the double-CEA MFC

The start-up of double-CEA MFC had been difficult due to the oxygen cross-over through the thin porous fabric material.<sup>12</sup> Several strategies had been applied initially to ensure start-up including autoclaving the medium solution to remove oxygen, a shorter HRT (4 min) to ensure lower oxygen level in the reactor, and the use of 2-layers of J-cloth to reduce oxygen diffusion.<sup>12</sup> In this study, however, the start-up of the larger CEA-MFC was much faster and easier, despite the much thinner, single non-woven cloth layer (about 0.3 mm) and much longer HRT (>75 min). As demonstrated in Fig.2, in less than 5 days the MFC generated a stable high power density of 1.8 kW m<sup>-3</sup>. This power density was much higher than the 1.01 kW m<sup>-3</sup> and 1.55 kW m<sup>-3</sup> generated by smaller CEA-MFCs containing 100 mM phosphate buffer and 200 mM bicarbonate buffer, respectively.<sup>5,12</sup>

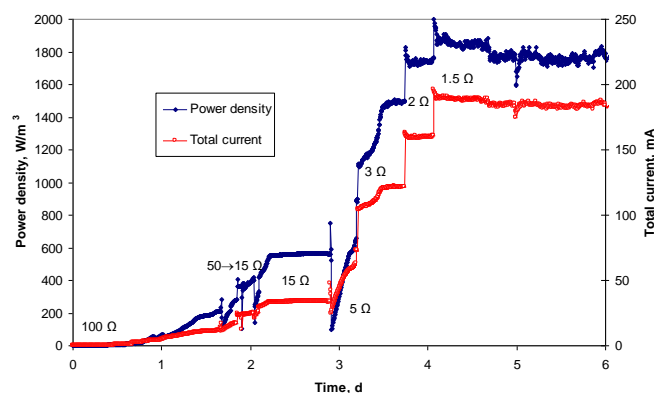


**Fig. 2** Fast start-up of large double CEA MFC. Power densities (solid square) are based on liquid volume and total current (open circle) is the sum of the current produced by both CEAs.

The surprisingly faster and easier start-up, in the large double CEA-MFC with the thinner separators, suggests that the anodic biofilm may be able to tolerate high levels of dissolved oxygen. To investigate oxygen tolerance of the exoelectrogens on the anode, oxygen was directly pumped into the MFC chamber between the two anodes at a speed of 20 ml/min through the recirculation tube for more than a day. The power density decreased from ~1700 W m<sup>-3</sup> to ~1400-1600 W m<sup>-3</sup> after pumping the air into the MFC and recovered in about a day after the air pump was stopped (Fig. 3). The fluctuation in power generation was possibly due to the much faster air flow (20 ml/min) than liquid flow (0.4 ml/min), which might affect the substrate availability to the anodes, especially to the anode at the top of the reactor. This result confirms that the mixed bacterial culture can tolerate high levels of oxygen in the water and even direct contact with air. This was possibly due to the continuous evolution of oxygen tolerant exoelectrogens under high oxygen levels for several years in our lab. The high oxygen level in the double-cathode MFC may help to inhibit methanogenesis and hydrogenesis. No CH<sub>4</sub> or H<sub>2</sub> production was detected during the 63-day operation and CO<sub>2</sub> was the only biogas produced.

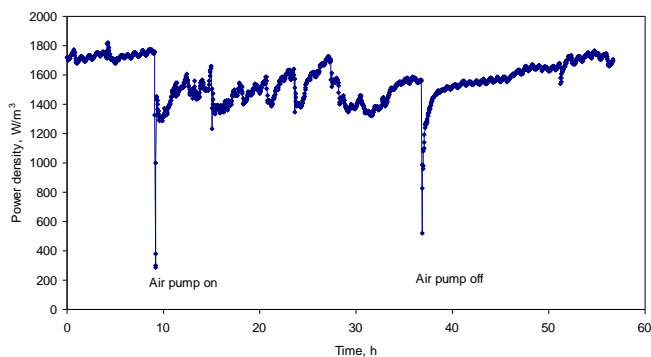


**Fig. 3** Oxygen tolerance of the anodic biofilm. The performance of CEA MFC was not significantly affected by the directly pumping of air in a speed of 20 ml/min and resumed quickly after the air pump was stopped.

### Effects of hydraulic retention time and recirculation

While the power density of CEA2 was stabilized at  $1.60 \pm 0.14 \text{ W m}^{-2}$ , the power density of CEA1 reached a maximum of  $4.30 \text{ W m}^{-2}$  ( $16.4 \text{ A m}^{-2}$ ) at an HRT of 1.37 h (Fig. 4), which was more than double the  $1.8 \text{ W m}^{-2}$  produced in the small MFC with similar reactor architecture and buffer strength.<sup>12</sup> Power densities were over  $4 \text{ W m}^{-2}$  with HRT in the range of 0.7-2.4 h, but decreased considerably outside this range (Fig. 5). The high current densities contribute to the high CE, which is in the range of 74-98% at the tested HRTs (Fig. 5A). The removal of the recirculation bottle increased the CE from 74% to 80% while slightly decreasing the power density by 4%. The complete removal of recirculation significantly decreased the power density by 21%, although the CE was further improved to 85%. These results demonstrate the importance of recirculation, which may enhance the mass transport of substrate to the electrode in this type of MFC reactor. On the other hand, the oxygen diffusion and other non-current-generating process might be affected by recirculation as well, resulting in a slightly lower CE.

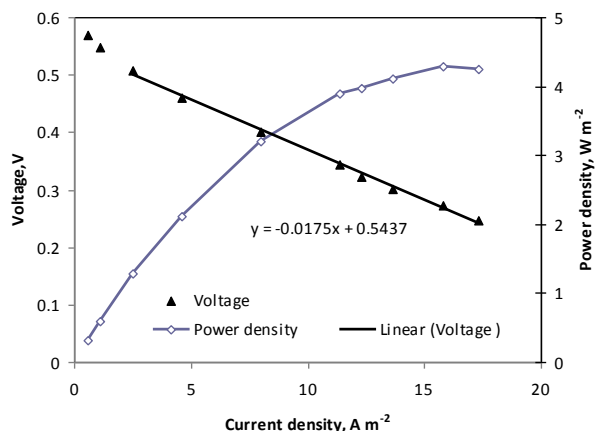


**Fig. 4** Polarization curves of CEA1 with 0.1 M phosphate and 0.1 M acetate at an HRT of 1.37 h. The linear fitting indicates the portion of curve used for internal resistance calculation.

Increased HRT resulted in increased acetate consumption, as

expected (Fig. 5B). Increased HRT also resulted in higher effluent pH, indicating higher  $\text{CO}_2$  release at longer HRTs (Fig. 5B). The absence of recirculation slightly decreased the effluent pH and acetate removal, probably due to the reduction in power density and current density (Fig 5).

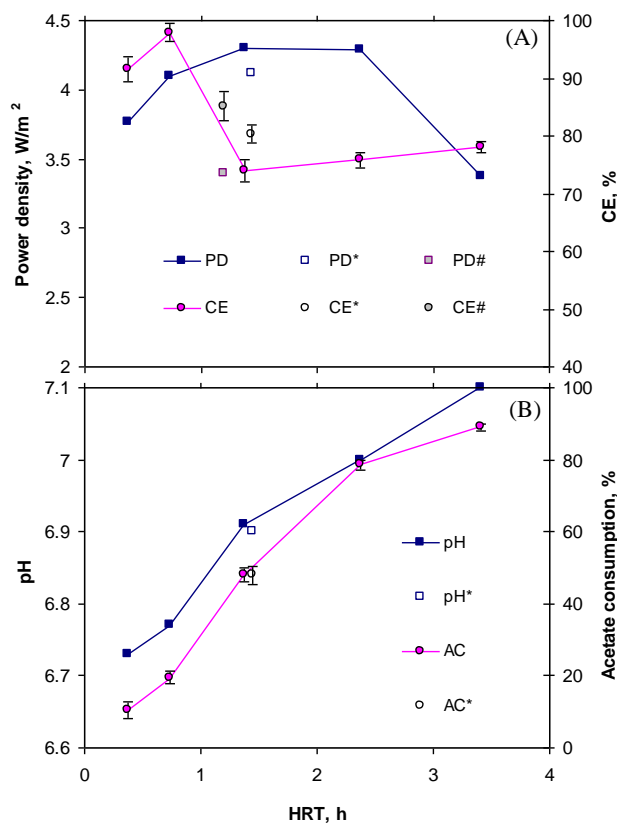


**Fig.5** Effects of hydraulic retention time on (A) power density (PD) based on CEA1 and coulombic efficiency (CE) and (B) on pH and acetate consumption (AC). \*Unfilled square and circle indicate PD and CE without the recirculation bottle. #Partially filled square and circle indicate PD and CE without the recirculation.

### Effects of phosphate buffer, acetate concentration and HRT

Buffer concentration plays a major role in facilitating proton transport from anode to cathode in an MFC, greatly affecting the internal resistance, and thus the performance of an MFC.<sup>5,15</sup> The production of  $\text{CO}_2$  in an MFC may increase the concentration of bicarbonate, another effective proton carrier, thus lowering the internal resistance and enhancing the power density.<sup>5,16,17</sup>

As demonstrated in Table 1, the power density of the MFC with 50 mM phosphate buffer increased 5% to  $3.40 \text{ W m}^{-2}$  when the acetate concentration increased from 100 mM to 150 mM at HRT of 1.22-1.28 h. It further increased 9% to  $3.70 \text{ W m}^{-2}$  ( $13 \text{ A m}^{-2}$ ) when HRT increased from 1.22 h to 3.00 h with acetate concentration of 150 mM. Such a power density is about 3 times of that produced in the small MFC with 50 mM phosphate buffer and 30 mM acetate. The power density increased 11% with the increase of buffer concentration from 50 to 100 mM. Further increasing the phosphate concentration to 200 mM only resulted in a 5% increase to a maximum of  $4.32 \text{ W m}^{-2}$ . The increase in power density was much smaller compared with the 45% and 11% observed in the small CEA-MFC when the buffer



concentration was increased from 50 to 100 and 200 mM, respectively.<sup>5</sup> Such results suggest the role of self-produced bicarbonate in reducing the internal resistance and enhancing the power generation. Although the contribution of self-produced bicarbonate might be negligible at low acetate concentrations and

short HRTs<sup>18</sup>, the contribution can be greatly enhanced through the manipulation of operating conditions. The accumulation of self-produced bicarbonate at higher influent acetate concentration and a longer HRT also resulted in elevated effluent pH possibly due to the release of CO<sub>2</sub> at elevated bicarbonate concentration.

**Table 1** Effects of phosphate buffer, acetate concentration and HRT on effluent pH, internal resistance and maximum power density based on CEA1, in comparison with the small MFC

	Phosphate buffer (mM)	Acetate concentration (mM)	HRT (h)	pH	Specific internal resistance (ohm cm <sup>2</sup> )	Max. power density (W m <sup>-2</sup> )
Large MFC	50	100	1.28	6.78	234	3.25
	50	150	1.22	7.09	230	3.40
	50	150	3.00	7.39	208	3.70
	100	100	1.44	6.90	187	4.12
	200	100	1.20	6.68	174	4.32
Small MFC <sup>5</sup>	50	30	0.1	6.80	480	1.25

## Discussion

### Enhanced performance of larger CEA-MFC

Scale-up is necessary for the commercial application of MFC technology, especially for wastewater treatment. Unfortunately, the scale-up of MFCs often leads to significant reduction in power density.<sup>6</sup> However, in this study, the maximum power density of a CEA-MFC increased from 1.8 to 4.3 W m<sup>-2</sup> despite the increase in electrode area by a factor of fourteen (Table 2). Such a power density is about 1 order of magnitude higher in comparison with liter-scale MFCs (Table 2). The specific cathode area (667 m<sup>2</sup>/m<sup>3</sup>) of the CEA-MFC is also much higher than those (100 m<sup>2</sup>/m<sup>3</sup> or less) of the liter-scale MFCs (Table 2). The higher power density based on cathode area and higher cathode specific area of the CEA-MFC resulted in 2-4 orders magnitude higher volumetric power density (Table 2). Although the volume (30 ml) of the MFC in this study is 2-3 orders of magnitude smaller than the liter-scale MFCs in many other studies, it produced comparable or even higher total power output of 62.3 mW (Table 2). The total power and power density could have been 86 mW and 2.87 kW m<sup>-3</sup>, respectively, if CEA2 had produced the same power as CEA1. Moreover, the CE of the CEA-MFC in this study is also considerably higher than the liter-scale MFCs.

The U-shaped titanium wires used as current collectors in the larger CEA-MFC created about 4 times larger contact area per electrode area than in the smaller CEA-MFC and might contribute to the reduction in internal resistance, thus improving performance. Other factors that might also contribute to the improved performance include the use of thin and high-flux separator material, the development of oxygen tolerant anodic biofilm, and the enhanced self-production of bicarbonate buffer..

### Electrode spacing: a limiting factor of MFC performance

The cathode is widely considered as the key factor limiting air-cathode MFC performance even with platinum as the catalyst. However, the membrane and/or electrolyte often contribute most to the internal resistance.<sup>14</sup> For example, the electrolyte contributes 78.2% of the internal resistance for a common air cathode, single-chamber MFC (1.7 cm anode-cathode spacing, 50 mM phosphate buffer). In comparison, the cathode and the anode only contribute 19.5% and 2.2%, respectively.<sup>14</sup> Therefore, the most effective way to enhance the performance of this kind of MFC is to reduce the electrolyte resistance, which can be achieved by reducing the anode-cathode spacing and/or increasing the pH buffer concentration.<sup>14</sup>

Reducing electrode spacing can proportionally decrease the area-specific electrolyte resistance and in turn the internal resistance, thus enhancing the performance of MFCs.<sup>14</sup> Moreover, reducing electrode spacing can increase the ratio of the electrode surface area/volume and in turn the maximum volumetric power density. However, possible short circuit and increased oxygen diffusion limit the minimum electrode spacing of membrane-less MFCs to about 1-2 cm,<sup>19</sup> which is still too large to keep the electrolyte resistance low. Membrane electrode assembly (MEA), a sandwich structure used in PEM fuel cells, can effectively minimize the electrode spacing and enhance MFC performance in comparison with other designs.<sup>20</sup> However, the inclusion of a cation exchange membrane (CEM), such as Nafion 117, needs to be carefully considered due to its high area-specific resistance at neutral pH conditions, which could be about 3000 Ω cm<sup>2</sup> and contribute 38-86% of the total internal resistances of two-chamber MFCs.<sup>14,21</sup> The major reason for the high resistance of the CEM in an MFC is the neutral pH condition, or extremely low proton concentration. CEM blocks the diffusion of proton carriers (phosphate and/or bicarbonate), resulting in a high cross-membrane pH gradient and resistance.<sup>5</sup>

**Table 2** Performance of the CEA MFC in comparison with liter-scale air cathode MFCs

MFC type	Anode material	Cathode material	Separator material	Volume (L)	Specific cathode area $\text{m}^2 \text{m}^{-3}$	Current density at max. power density ( $\text{A m}^{-2}$ )   ( $\text{A m}^{-3}$ )		Max. Power Density ( $\text{W m}^{-2}$ )   ( $\text{W m}^{-3}$ )		Max. power (mW)	CE (%)	Reference
Double CEA	Carbon cloth	Carbon cloth/Pt	None-woven Cloth	0.030	667	16.4*	7600 <sup>#</sup>	4.30*	2080 <sup>#</sup>	62.3 <sup>#</sup>	74-98	This study
Double CEA	Carbon cloth	Carbon cloth/Pt	J-Cloth	0.0025	560	9.0	5000	1.80	1010	2.5	-	12
Tubular	Carbon veil	Carbon cloth/Pt	CMI-7000	1	43	0.6	24	0.13	5.6	5.6	-	8
Bipolar	Ti plate w/ MMO	Ti plate w/ MMO	Biopolar membrane	20	100	0.3	30	0.11	11	220	-	22
Biocathode	Carbon felt	Carbon felt	CMI-7000	7.2	5.6	2	10	0.77	4.3	31	10-50	10
Double MEA	Carbon paper	Carbon cloth/Pt	Nafion	1.5	21	0.3	5	0.16	3.5	5.3	5	11
Multiple electrode	GAC	Carbon cloth/Pt	NA	20	0.3	2	0.5	0.38	0.2	3.4	0.04-0.3	7
Biocathode	granular graphite	Carbon felt	CMI-7000	7.5	25	0.8	20	0.39	9.8	74	~ 50	9

\*for CEA1; <sup>#</sup>for the double-CEA MFC; .

The proton transport from anode to cathode can be greatly enhanced by replacing the CEM with a porous fabric material, resulting in a CEA structure. In a CEA-MFC using phosphate buffer, the proton transfer rate is limited by the  $\text{H}_2\text{PO}_4^-$  diffusion rate, which can be calculated based on Fick's Law.<sup>5</sup> For example, the maximum current density for a CEA-MFC with 0.6 mm electrode spacing (2 layers of J-cloth) and 0.1 M phosphate buffer at 30°C is 10  $\text{A m}^{-2}$ , assuming the effective diffusion coefficient in J-cloth is 60% of that in water.<sup>5</sup> Such a current density is very close to the actual maximum current density produced in that study. Therefore, the proton diffusion rate may indeed determine the maximum current density, which can be enhanced by increasing buffer concentration or reducing electrode spacing (or separator thickness). In this study, the maximum current density almost doubled to about 20  $\text{A m}^{-2}$  with a 50% thinner separator material (0.3 mm non-woven cloth), further demonstrating the importance of electrode spacing on MFC performance.

The increased electrode spacing, due to the biogas produced between the anode and cathode, was considered to be the major reason for the reduced performance for CEA2. Two types of gas releasing openings were used in this study. The 1 cm by 1 cm crosses seem more effective than the  $\Phi 0.3$  cm holes based on the performance of the two CEAs and open-cell examination, probably because the cross opening is much larger.

#### Separator material: critical for the cost and performance of MFCs

In addition to electrically insulating the anode and cathode, reducing oxygen crossover is considered a major function of separators in MFCs. The elimination of the membrane in separator-free single chamber air-cathode MFCs not only reduces the cost and complexity of MFCs, but also increases the power density due to a decrease in internal resistance.<sup>23</sup> However, the higher oxygen diffusion in a separator-free system results in

lower CE. The oxygen crossover can be effectively suppressed by a low-cost cloth layer in a CEA-MFC.<sup>12</sup> The anode-cathode spacing was reduced to less than 1 mm, significantly enhancing the power density while improving the CE at the same time. Two layers of J-cloth (0.6 mm in thickness) were used in CEA-MFCs in our previous studies to balance the oxygen diffusion and proton mass transfer.<sup>5,12</sup> The thickness of separator can be further reduced with the development of an oxygen tolerant anodic biofilm (Fig.3). In this study, a single 0.3 mm thick non-woven cloth was used as the separator, further reducing the internal resistances caused by the separator and electrolytes, and more than doubling the power generation. The non-woven cloth, containing 25% polyester, has excellent physical strength as well as chemical and biological stability. No sign of degradation is observed in more than 4 years of application of this material in the MFCs in our lab.

#### High current density, high Coulombic efficiency

A side effect of a thinner separator and reduced electrode spacing is increased oxygen crossover, which may lead to the growth of oxygen consuming heterotrophs. Although the exoelectrogens can still outcompete the other heterotrophs, demonstrated by the fast MFC start-up (Fig. 2) and high oxygen tolerance of anodic biofilms (Fig. 3), the higher oxygen crossover may lead to decreased CEs. However, the high CEs ( $83.5 \pm 10.6\%$ ) achieved in this study indicated otherwise. This might be due to the high current density achieved in the CEA-MFC. The maximum oxygen flux through a 0.3 mm thick water layer at 30°C is  $1.2 \mu\text{mol m}^{-2} \text{S}^{-1}$  based on Fick's Law,<sup>12</sup> or an equivalent current density of 0.42  $\text{A m}^{-2}$ , assuming no oxygen at the anode and the effective diffusion coefficient in non-woven cloth is 60% of that in water. This is only 2.5% of the current density (16.4  $\text{A m}^{-2}$ ) at which maximum power density was produced in this study and 2% of the maximum proton flux (20  $\text{A m}^{-2}$  equivalent) via 0.1 M

phosphate buffer under the same assumption. The oxygen flux can be even lower if the oxygen level at the anode is not zero, which reduces the concentration difference across the separator. Although the actual oxygen level might be higher due to biofilm development at the cathode and the porous separator, a CE of over 95% can be expected if oxygen is the only sink of non-current-generating substrate consumption. The relatively lower actual CEs ( $83.5 \pm 10.6\%$ ) in this study indicated that the substrate consumption in the recirculation line and for biomass synthesis should also be considered. Nevertheless, high CEs are possible even with a low mass transfer resistance separator as thin as 0.3 mm. Therefore, oxygen crossover shouldn't be a major consideration in the selection of separator materials if the anodic biofilm is oxygen tolerant and the current density is greater than  $15 \text{ A m}^{-2}$ .

## Outlook

The high performance of the double CEA-MFC holds great meaning for the potential application of MFC technology. The possible maximum power density of  $2.87 \text{ kW m}^{-3}$  is more than two-times higher than the power of  $1.1 \text{ kW m}^{-3}$  that can be produced in anaerobic digestion, based on a conversion rate of  $25 \text{ kg COD m}^{-3} \text{ d}^{-1}$  and an overall energy efficiency of 30%.<sup>24</sup> Based on a voltage efficiency of 25% and CE of 83.5%, the energy efficiency of the MFC at maximum power was only 21%, which is lower than that of anaerobic digestion (28-30%).<sup>1,24</sup> The energy efficiency, however, can be significantly increased if the MFC had been operated at a higher voltage. For example, the energy efficiency can be increased to a comparable 30% if the MFC had been operated at 0.4 V, or 35% at 0.46 V. According to the polarization curves (Fig. 4), the power densities of  $2.13 \text{ kW m}^{-3}$  at 0.4 V and  $1.41 \text{ kW m}^{-3}$  at 0.46 V were still much higher than that of anaerobic digestion. In addition to the higher power at comparable energy efficiency, MFCs also hold advantages over anaerobic digestion for their simplicity, as electricity is directly generated. The removal of  $\text{H}_2\text{S}$  from the biogas produced from methanogenesis to prevent combustion-associated byproducts is expensive and energy intensive.<sup>25</sup> Additional energy may be needed to strip  $\text{CH}_4$  from the effluent to prevent the dissolved  $\text{CH}_4$  from escaping into the atmosphere<sup>1</sup>, which is over 20 times more effective in trapping heat in the atmosphere than  $\text{CO}_2$ . Furthermore, the oxygen tolerant biofilm makes it possible to operate MFCs at high anodic oxygen levels. This not only eliminates the possibility of producing  $\text{H}_2\text{S}$  and  $\text{CH}_4$  in MFCs, but also diversifies pollutant degradation pathways, thus making MFCs more effective at pollution removal than anaerobic processes.

At an overall energy efficiency comparable to anaerobic digestion, MFC technology has great potential in converting wastewater treatment from an energy consumer to a net energy producer. The energy needs for a typical domestic wastewater treatment plant employing aerobic activated sludge treatment and anaerobic sludge digestion is  $0.6 \text{ kWh m}^{-3}$ , about half of which is for electrical energy to supply air for the aeration basins.<sup>1</sup> With air-cathode MFCs using passive aeration, the energy need can be reduced to  $0.3 \text{ kWh m}^{-3}$ , assuming the same energy is required for other processes. The energy content in a typical  $500 \text{ mg COD l}^{-1}$  domestic wastewater has been estimated as  $1.93 \text{ kWh m}^{-3}$ , of which  $1.23 \text{ kWh m}^{-3}$  is biodegradable.<sup>1</sup> A net energy of 0.07

$\text{kWh m}^{-3}$  could be produced with air-cathode MFCs, assuming 30% of the biodegradable COD in domestic wastewater can be converted to electricity. The actual net energy might be much higher than the estimation, as a recent study demonstrated the actual energy value in wastewater might have been substantially underestimated.<sup>26</sup> Much higher net energy may be produced from high strength industrial wastewater, especially food processing wastewater.

The current densities, up to  $20 \text{ A m}^{-2}$ , obtained in this study are considerably higher than the equivalent current densities of most biofilm processes, including aerobic heterotrophic biofilms ( $1.6\text{--}2.8 \text{ A m}^{-2}$ ) and methanogenic biofilms ( $0.5\text{--}9.5 \text{ A m}^{-2}$ ).<sup>27</sup> The higher current density demonstrates the competitive advantage and great potential of microbial electrochemical technology. The higher current density indicates higher COD removal rate for wastewater treatment. The current density of  $16.4 \text{ A m}^{-2}$  ( $10.9 \text{ kA m}^{-3}$ ) can be translated to a conversion rate of  $78.1 \text{ kg COD m}^{-3} \text{ d}^{-1}$  to current, or a total of  $93.5 \text{ kg m}^{-3} \text{ d}^{-1}$  COD removal rate assuming the CE is 83.5%. This is almost 3 times higher than the  $25 \text{ kg COD m}^{-3} \text{ d}^{-1}$  of an anaerobic digester, demonstrating the high efficiency of MFCs in pollution removal.

A major challenge of commercial application of MFC technology in wastewater treatment is the high capital cost, especially material cost of anodes, cathodes, and separators. The capital cost of the laboratory MFC in this study for wastewater treatment is estimated to be  $\$3/\text{kg COD}$ , assuming  $\$1500/\text{m}^2$  for cathode,  $\$100/\text{m}^2$  for anode,  $\$1/\text{m}^2$  for separator, and  $\$5000/\text{m}^3$  for reactor and others, and a lifetime of 10 years. The anode is a non-limiting factor in the current stage of MFC development. The current commercial price for carbon cloth is about a few dozen dollars/ $\text{m}^2$ , which is expected to be reduced when large scale application of this material in MFCs is possible. Further development of anode material should further reduce cost. The cathode is a major limiting factor of MFCs, both in performance and cost. The carbon cloth/Pt cathode is over  $\$1000/\text{m}^2$  based on materials used in the laboratory systems. However, it is possible to find some cathode materials suitable for the neutral pH and relatively low current density. Activated carbon provides a good example of low-cost high-performance cathode materials.<sup>28</sup>

Assuming the further costs can be reduced to  $\$50/\text{m}^2$  for cathode,  $\$10/\text{m}^2$  for anode,  $\$0.2/\text{m}^2$  for separator, and  $\$5000/\text{m}^3$  for reactor and others, the capital cost of wastewater treatment will be  $\$0.1/\text{kg COD}$  for full-scale MFCs with performance similar to the MFC in this study and a lifetime of 10 years. Such a capital cost is comparable with that of traditional activated sludge process.<sup>29</sup> The capital cost can be further reduced with longer lifetime of the reactor and/or with material recycling. The capital cost can also be offset by reduction in operation cost and revenue from electricity production<sup>29</sup>, making it more competitive than traditional activated sludge process.

It should be noted that there are still challenges in directly operating MFCs using real wastewater. For example, both BOD and buffer concentrations in domestic wastewater are much lower than those in this study. Evaluating the performance of the CEA-MFCs using real wastestreams and addressing the possible issues, such as water distribution and clogging of reactors are necessary. Future studies on further scale-up and enhancing the self-produced bicarbonate buffer are also needed.

## Acknowledgements

The authors acknowledge support from the U.S. National Science Foundation (CBET 0955124) and help from Cheng Li for analyzing the acetate samples.

## Notes

<sup>a</sup> Department of Biological and Ecological Engineering, Oregon State University, 116 Gilmore Hall, Corvallis, OR 97331, U.S.A

Fax: 541 737 2082; Phone: 541 737 6309; Email: [liuh@engr.orst.edu](mailto:liuh@engr.orst.edu)

<sup>b</sup> Department of Environmental Health, Korea National Open University, Seoul, KOREA

† Electronic Supplementary Information (ESI) available: Detailed procedure for preparing polarization curves and effects of water pressure and electrode location on MFC performance. See DOI: 10.1039/b000000x/

## References

- 1 P.L. McCarty, J. Bae, and J. Kim, *Environ. Sci. Technol.*, 2011, **45**, 7100–7106.
- 2 I. Shizas and D.M., *J. Energy Eng.*, 2004, **130** (2), 45–53.
- 3 B.E. Logan, P. Aelterman, B. Hamelers, R. Rozendal, U. Schröder, J. Keller, S. Freguic, W. Verstraete and K. Rabaey. *Environ. Sci. Technol.*, 2006, **40**(17), 5181–5192.
- 4 H. Liu, R. Ramnarayanan and B.E. Logan, 2004, *Environ. Sci. Technol.*, **38**, 2281–2285.
- 5 Y. Fan, H. Hu and H. Liu, 2007, *Environ. Sci. Technol.*, **41**, 8154–8158.
- 6 A. Dewan, H. Beyenal and Z. Lewandowski, *Environ. Sci. Technol.* 2008, **42**, 7643–7648.
- 7 D. Q. Jiang, M. Curtis, E. Troop, K. Scheible, J. McGrath, B. X. Hu, S. Suib, D. Raymond and B. K. Li, *Int. J. Hydrogen Energy*, 2011, **36**, 876–884.
- 8 J. R. Kim, J. Rodriguez, F. R. Hawkes, R. M. Dinsdale, A. J. Guwy and G. C. Premier, *Energy Environ. Sci.*, 2011, **4**, 459–465.
- 9 P. Clauwaert, S. Mulenga, P. Aelterman and W. Verstraete, *Appl. Microbiol. Biotechnol.* 2009, **83**, 241–247.
- 10 P. Liang, M. Fan, X. Cao and X. Huang, *J. Chem. Technol. Biotechnol.*, 2009; **84**: 794–799.
- 11 Z. Li, L. Yao, L. Kong and H. Liu, *Bioresour. Technol.*, 2008, **99**, 1650–1655.
- 12 Y. Fan, H. Hu and H. Liu, 2007, *J. Power Sources*, 171 (2) 348–354.
- 13 D.R. Lovley and E.J.P. Phillips, *Appl. Environ. Microbiol.*, 1988, **54**, 1472–1480.
- 14 Y. Fan, E. Sharbrough and H. Liu, *Environ. Sci. Technol.*, 2008, **42**, 8101–8107
- 15 H. Liu, S. Cheng, B.E. Logan, *Environ. Sci. Technol.*, 2005, **39**, 5488–5493.
- 16 C. I. Torres, A. K. Marcus and B. E. Rittmann, *Biotechnol. Bioeng.*, 2008, **100**, 872–881.
- 17 J. J. Fornero, M. Rosenbaum, M. A. Cotta and L. T. Angenent, *Environ. Sci. Technol.*, **44**, 2728–2734.
- 18 Y. Fan, H. Hu and H. Liu, 2008, *Environ. Sci. Technol.*, **42**, 6306.
- 19 S. Cheng, H. Liu and B.E. Logan, *Environ. Sci. Technol.*, 2006, **40**, 2426–2432.
- 20 P. Liang, X. Huang, M.-Z. Fan, X.-X. Cao, C. Wang, *Applied Microb. Biotech.*, 2007, **77** (3), 551–558.
- 21 H. Liu and Y. Fan. “Electrode Materials for Microbial Fuel Cells” in *Materials in Low Temperature Fuel Cells*. Bradley Ladewig. Wiley. 2012
- 22 A. Dekker, *Environ. Sci. Technol.* 2009, **43**, 9038–9042.
- 23 H. Liu and B.E. Logan, *Environ. Sci. Technol.*, 2004, **38**, 4040 – 4046.
- 24 A. Ter Heijne, F. Liu, L. S. van Rijnsoever, M. Saakes, H.V.M. Hamelers, C.J.N. Buisman, *J. Power Sources*, 2011, **196**, 7572– 7577.
- 25 B.E. Rittmann, C.I. Torres and A.K. Marcus, Understanding the distinguishing features of a microbial fuel cell as a biomassbased renewable energy technology. *Emerging Environmental Technologies* (V. Shah, ed), pp. 1–28. Springer, New York. 2008
- 26 E.S. Heidrich, T.P. Curtis, J. Dolfig, *Environ. Sci. Technol.* 2011, **45**, 827–832.

- 27 C.I. Torres, A.K. Marcus, H.-S. Lee, P. Parameswaran, R. Krajmalnik-Brown and B.E. Rittmann, *FEMS Microbiol. Rev.*, 2010, **34**, 3–17
- 28 F. Zhang, S. Cheng, D. Pant, G.V. Bogaert and B.E. Logan, *Electrochem. Comm.*, 2009, **11**, 2177–2179
- 29 R.A. Rozendal, H.V. Hamelers, K. Rabaey, J. Keller and C.J. Buisman, *Trends Biotechnol.*, 2008. **26**, 450–459.